Plasmonic lipogels: driving co-assembly of composites with peptide-based gels for controlled drug release

Sérgio R. S. Veloso[a], Valéria Gomes[a,b], Sérgio L. F. Mendes[a], Loic Hilliou[c], Renato B. Pereira,[d] David M. Pereira,[d] Paulo J. G. Coutinho[a], Paula M. T. Ferreira[b], Miguel A. Correa-Duarte[e], and Elisabete M. S. Castanheira[a,*]

[a] Physics Centre of Minho and Porto Universities (CF-UM-UP) and LaPMET Associate Laboratory, University of Minho, Campus de Gualtar, 4710-057 Braga, Portugal.

[b] Centre of Chemistry (CQUM), University of Minho, Campus de Gualtar, 4710-057 Braga, Portugal.

[c] Institute for Polymers and Composites, Department of Polymer Engineering, University of Minho, Campus de Azurém, 4800-058 Guimarães, Portugal.

[d] REQUIMTE/LAQV, Lab. of Pharmacognosy, Department of Chemistry, Faculty of Pharmacy, University of Porto, R. Jorge Viterbo Ferreira, 228, 4050-313 Porto, Portugal

[e] CINBIO, Universidad de Vigo, 36310 Vigo, Spain.

Supplementary Information

Preparation of liposomes formulations

Liposomes fabricated with 10% or 30% of DPPE or cholesterol through the ethanolic injection method displayed slight changes in the hydrodynamic diameter and zeta potential compared to the neat liposomes of DPPC, as well as the polydispersity index (Table S1). Besides, the close values of 1,6-diphenyl-1,3,5-hexatriene (DPH) fluorescence anisotropy indicate that the several formulations membranes display similar microfluidity, which further suggests that the composition may not strongly influence the release of the liposomes content, as the properties are similar.

Table S1. Hydrodynamic diameter (D_h), polydispersity index (PDI) and zeta potential of several liposome formulations (0.1 mM) at 25 °C in pH=7.4 phosphate buffer 10 mM. The steady-state fluorescence anisotropy (r) of 1,6-diphenyl-1,3,5-hexatriene (DPH) in the liposomal formulations is also included. SD stands for standard deviation (n = 3).

	$D_h \pm$ SD (nm)	PDI ± SD	Zeta potential ± SD (mV)	r ± SD
DPPC	218 ± 38	0.25 ± 0.04	-1.4 ± 0.7	0.33 ± 0.01
DPPC:DPPE 9:1	186 ± 47	0.23 ± 0.01	-1.8 ± 0.8	0.31 ± 0.01
DPPC:DPPE 7:3	199 ± 18	0.26 ± 0.01	-1.6 ± 0.9	0.27 ± 0.01
DPPC:Ch 9:1	196 ± 36	0.21 ± 0.03	-1.6 ± 0.9	0.29 ± 0.01
DPPC:Ch 7:3	175 ± 7	0.30 ± 0.05	-1.4 ± 0.6	0.29 ± 0.01

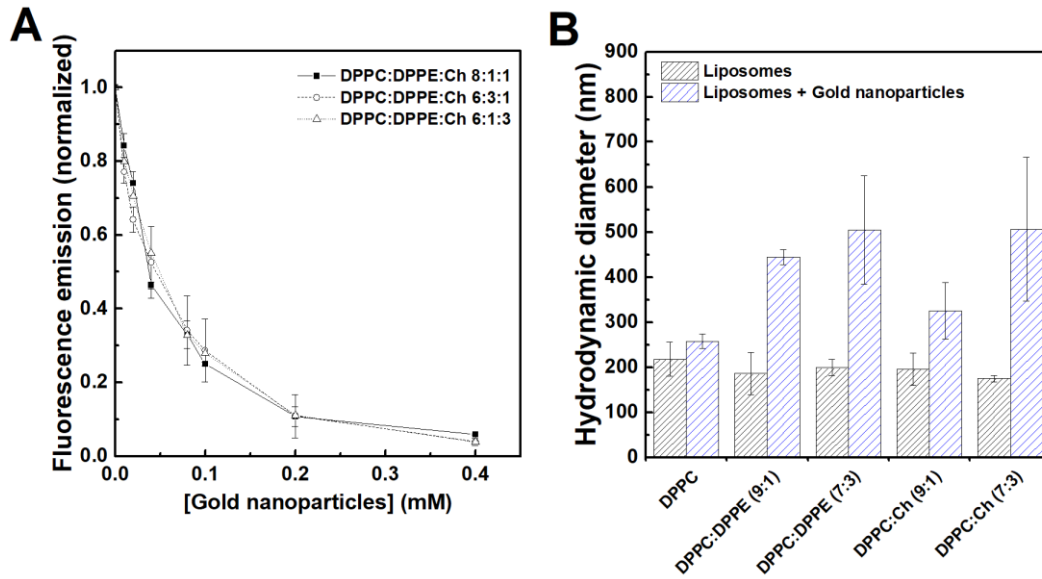# Adsorption of gold nanoparticles to liposome formulations

Figure S1. (**A**) Fluorescence emission of the supernatant after titration of NBD-labelled (0.2 µM, λ_{exc}= 450 nm) liposomes (0.1 mM) with gold nanoparticles (up to 0.4 mM gold ~ 4 nM nanoparticles for a size of 13 nm). (**B**) Hydrodynamic diameter of the liposomal formulations with and without nanoparticles. Data is represented as mean ± SD, and n = 3.

After each mixing and centrifugation, the fluorescence intensity of the supernatant was measured, which decreased owing to the deposition of the liposome-nanoparticle aggregates. Besides, the profiles were similar for all formulations, suggesting that varying the proportion of DPPE and cholesterol did not affect the adsorption of gold nanoparticles to liposomes surface (Figure S2A). This independence on the presence of cholesterol and DPPE can be associated with the strong interaction between the phosphocholine (PC) group and gold nanoparticles.[17-19] The PC group is roughly parallel to the liposome surface, which in the presence of negatively charged particles tilts to favour the interaction via the positively charged choline. Besides, the adsorption can also be associated to a strong van der Waals force between both colloids, as the adsorption of the particles has been demonstrated to still take place after incubation with free ions (citrate, choline and phosphate).[19]
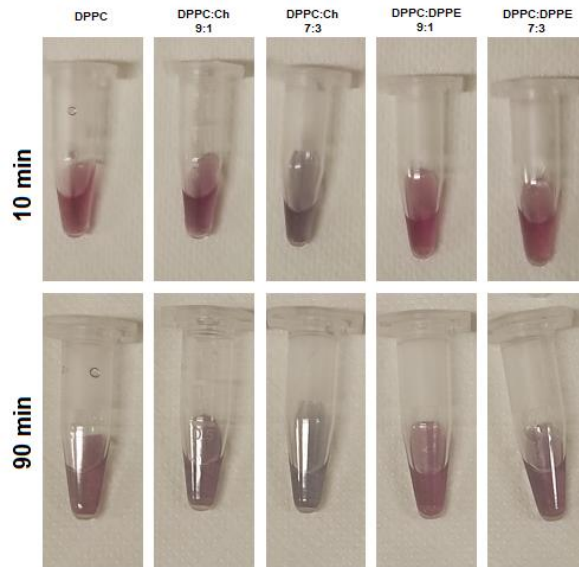
Figure S2. Images of gold nanoparticles combined with liposomes (lipid:gold 1:10), 10 min and 90 min after mixing.

The assembly of gold nanoparticles and liposomes has been explained to be influenced by both the kinetic and thermodynamic effects.[18] For instance, after adsorption of the citrate-stabilized gold nanoparticles to the DPPC membrane, the gold nanoparticles aggregation is proposed to be both kinetically and thermodynamically unfavourable as all the membrane is in the gel phase, which strongly limits the diffusion of the nanoparticle-liposome complexes due to the high viscosity, and also there are no fluid/gel interfaces to remove. These aggregates were demonstrated to be larger at low liposome concentration,[19] which can extend beyond a monolayer, as the collective van der Waals force of the formed clusters can strongly attract the individual nanoparticles.

Regarding the liposomes containing DPPE and cholesterol, based on the results, we propose that the fast aggregation can be potentially associated with the formation of domains by the particle-lipid complexes that favour the particle aggregation so to decrease the interface area between coexisting phases. In this sense, despite the similar particle adsorption, the formulations displayed different membrane dynamics, in which DPPE and cholesterol favoured particle aggregation.

Table S2. Hydrodynamic diameter (D_h) and polydispersity index (PDI) of several liposomes (0.1 mM) with gold nanospheres (0.4 mM gold) at 25 °C in pH=7.4 phosphate buffer 10 mM. The steady-state fluorescence anisotropy (r) of 1,6-diphenyl-1,3,5-hexatriene (DPH) is also included. SD stands for standard deviation (n = 3).

	$D_h \pm$ SD (nm)	PDI ± SD	r ± SD
DPPC	258 ± 16	0.252 ± 0.01	0.25 ± 0.02
DPPC:DPPE 9:1	445 ± 17	0.251 ± 0.01	0.25 ± 0.03
DPPC:DPPE 7:3	504 ± 120	0.273 ± 0.01	0.24 ± 0.02
DPPC:Ch 9:1	326 ± 63	0.253 ± 0.03	0.26 ± 0.04
DPPC:Ch 7:3	507 ± 160	0.290 ± 0.02	0.28 ± 0.01

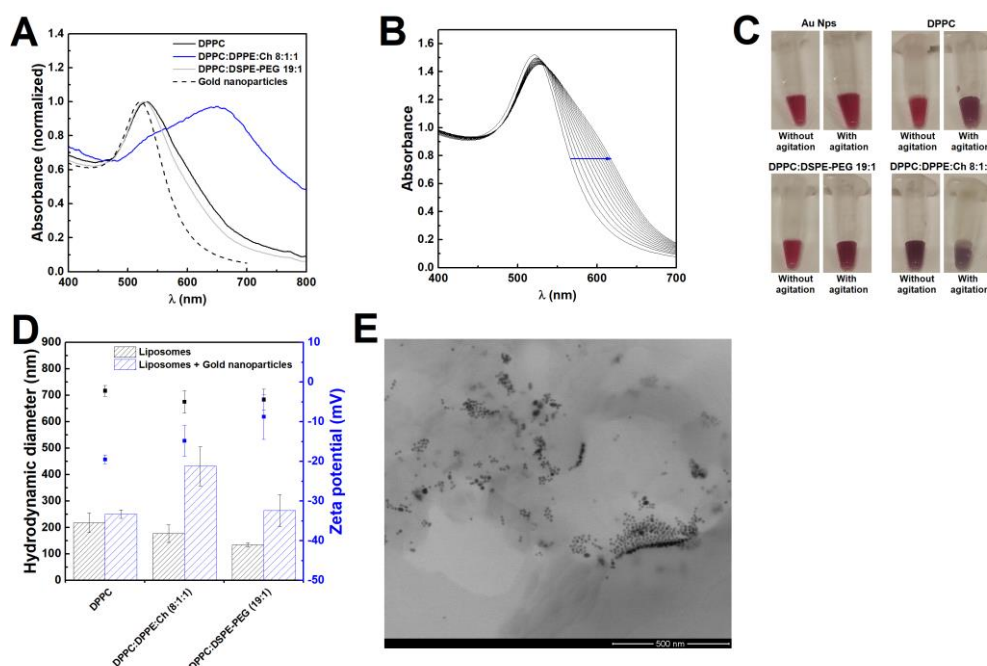# Adsorption of gold nanoparticles to selected liposome formulations

Figure S3. (**A**) Normalized absorption spectra of neat gold nanoparticles and 10 min after mixing with liposomes (lipid:gold 1:10). (**B**) Kinetics of aggregation of gold nanoparticles (0.4 mM gold) upon vigorous mixing with DPPC liposomes (0.1 mM) during 1 hour (the first spectrum is previous to vortexing). (**C**) Images of neat gold nanoparticles and combined with liposomes (lipid:gold 1:10) 10 min after mixing (before agitation) and 30 min after vortexing the same sample (after agitation). (**D**) Comparison of the hydrodynamic diameter (bar) and zeta potential (scatter) of the DPPC, DPPC:DPPE:Ch 8:1:1 and DPPC:DSPE-PEG 19:1 liposome formulations with and without gold nanospheres. Data is represented as mean ± SD, and n = 3. (E) STEM image of the DPPC:DPPE:Ch (8:1:1) (0.1 mM) liposomes after interaction with gold nanoparticles (0.4 mM) in which large nanoparticle aggregates are observed on the liposomes' membrane.

Mixing of the gold nanoparticles with liposomes also resulted in different equilibrium states that are displayed in figure S3A. Mainly, the DPPC:DPPE:Ch (8:1:1) liposomes quickly induced aggregation, which is in line with the effects observed for DPPE and Ch separately, while the DPPC and DPPC:DSPE-PEG (19:1) liposomes only induced a slight shift. However, subjecting the samples to vigorous vortexing was found to favour a quicker aggregation of gold nanoparticles (see aggregation kinetics with DPPC in figure S3B). In addition to the colour changes observed in Figure S3C before and after vortexing of the mixtures, the fast aggregation with the DPPC:DPPE:Ch (8:1:1) formulation led to the formation of large aggregates (see figure S3D and S3E).

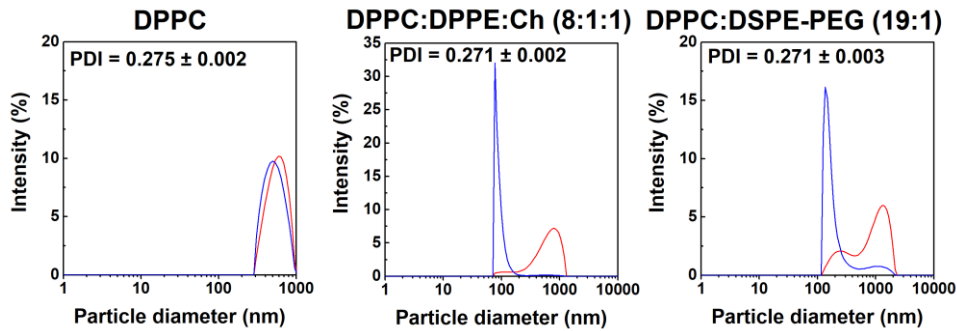# Effect of particle adsorption on the selected liposomes

Figure S4. Dynamic light scattering intensity-weighted (red) and number-weighted (blue) distributions of the liposome formulations with and without gold nanorods. The values of PDI are also included and is represented as mean ± SD, and n = 3.
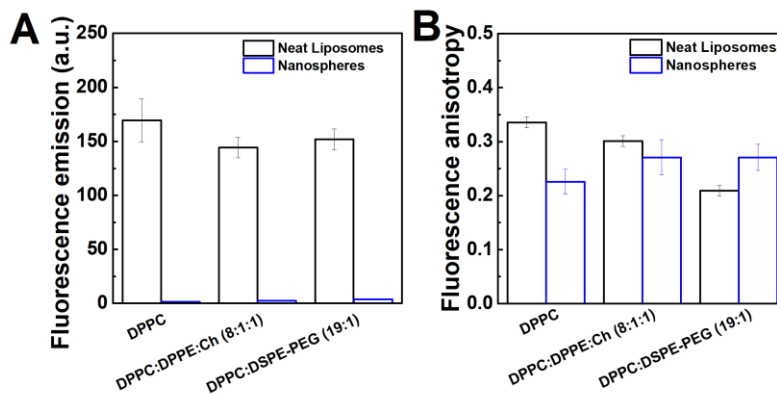

Figure S5. (**A**) Fluorescence emission and (**B**) fluorescence anisotropy of DPH (2 μM, λ_{exc}= 365 nm) in neat liposomes (0.1 mM) and after mixing with gold nanospheres (0.4 mM gold).

Opposed to the results obtained for the silica-coated gold nanorods, the gold nanospheres induced a strong fluorescence quenching (Figure S5A) and a decrease of the liposomes' membrane microviscosity (Figure S5B) as in previous formulations. However, as in silica-coated gold nanorods, a fluorescence anisotropy increase was obtained for the PEGylated formulation. In addition, the larger values of anisotropy obtained for the samples with nanospheres in the presence of peptide (Figure S5C) suggests that the peptide inhibits the nanoparticle-membrane interaction.

Table S3. Hydrodynamic diameter (D_h), polydispersity index (PDI) and zeta potential of the selected liposomes (0.1 mM) with gold nanospheres (0.4 mM gold) and nanorods coated with mesoporous silica (0.1 mg/mL) at 25 °C in pH=7.4 phosphate buffer 10 mM. The steady-state fluorescence anisotropy (r) of 1,6-diphenyl-1,3,5-hexatriene (DPH) is also included. SD stands for standard deviation (n = 3).

Liposome	Nanoparticle	D_h ± SD (nm)	PDI ± SD	Zeta potential ± SD (mV)	r ± SD
DPPC	Neat	218 ± 38	0.230 ± 0.002	-2.2 ± 1.3	0.34 ± 0.01
	NS	250 ± 16	0.257 ± 0.002	-19.5 ± 1.0	0.23 ± 0.02
	NR	738 ± 141	0.275 ± 0.002	-10.4 ± 0.6	0.33 ± 0.004
DPPC:DPPE:Ch 8:1:1	Neat	177 ± 33	0.181 ± 0.003	-5.0 ± 2.8	0.30 ± 0.01
	NS	431 ± 73	0.312 ± 0.004	-14.8 ± 3.9	0.27 ± 0.03
	NR	761 ± 218	0.271 ± 0.002	-11.9 ± 0.2	0.33 ± 0.003
DPPC:DSPE-PEG 19:1	Neat	135 ± 8	0.216 ± 0.004	-4.4 ± 2.6	0.21 ± 0.01
	NS	264 ± 61	0.262 ± 0.001	-8.8 ± 5.7	0.27 ± 0.02
	NR	1059 ± 241	0.271 ± 0.003	-23.1 ± 0.8	0.26 ± 0.004

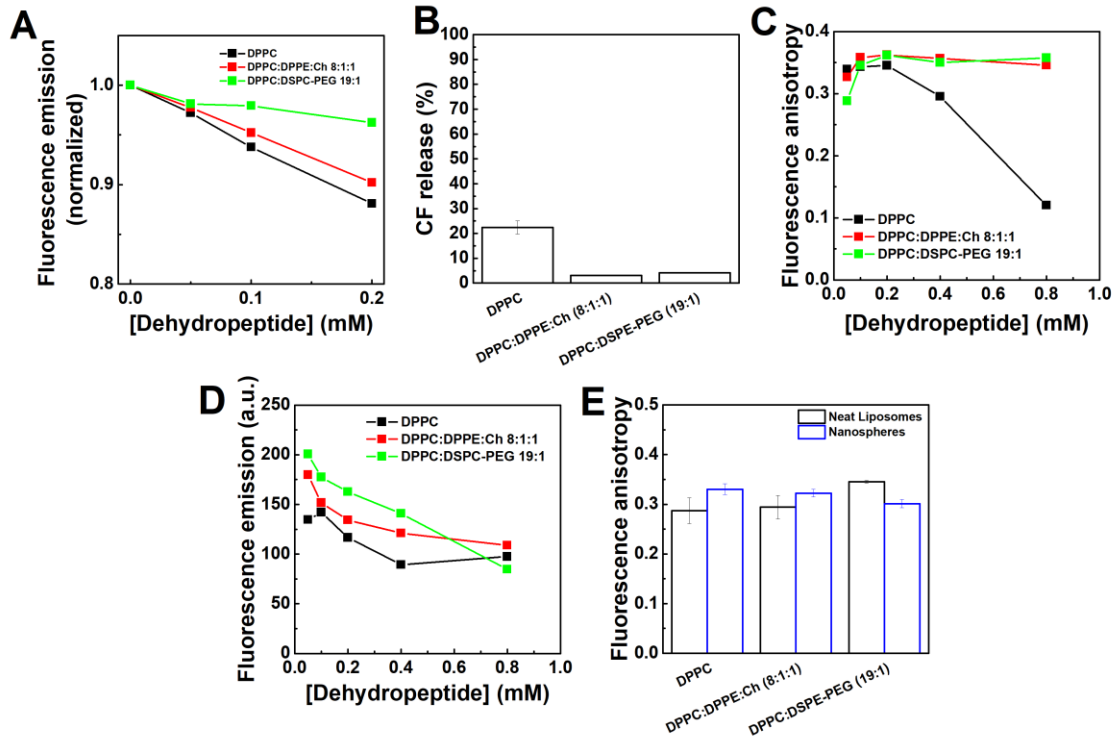# Fabrication of plasmonic lipogel formulations

Figure S6. (**A**) Normalized fluorescence emission of 5(6)-carboxyfluorescein (CF) loaded liposomes (0.1 mM) titrated with increasing concentration of dehydropeptide. (**B**) Release percentage of 5(6)-carboxyfluorescein loaded in liposomes of different composition to pH 7.4 phosphate buffer after 24 h. Data is represented as mean ± SD, and n = 3. (**C**) Fluorescence anisotropy and (**D**) fluorescence emission of DPH (2 μM, λ_{exc}= 365 nm) loaded liposomes (0.1 mM) titrated with dehydropeptide. (**E**) Fluorescence anisotropy of DPH (2 μM, λ_{exc}= 365 nm) in neat liposomes (0.1 mM) and after mixing with gold nanospheres (0.4 mM gold) in the presence of the dehydropeptide (0.1 mM). Data is represented as mean ± SD, and n = 3.

The release percentage from the liposomes in figure S6B further demonstrated that DPPC liposomes displayed a higher release than the other formulations.

The interaction of liposomes with the hydrogelator was accompanied by a decrease of DPH fluorescence anisotropy for neat DPPC liposomes, while it remained closely unchanged in the other formulations (figure S6C). This can be associated with the interaction of the peptide with the DPPC membranes, leading to the localization of DPH to a more fluid region of the membrane (the central region), which was also described to occur for other molecules interacting with liposomes containing DPH.[42] The titration with peptides was also accompanied by a decrease of DPH fluorescence emission (figure S6D), potentially due to inner filter effect from hydrogelator micelles.
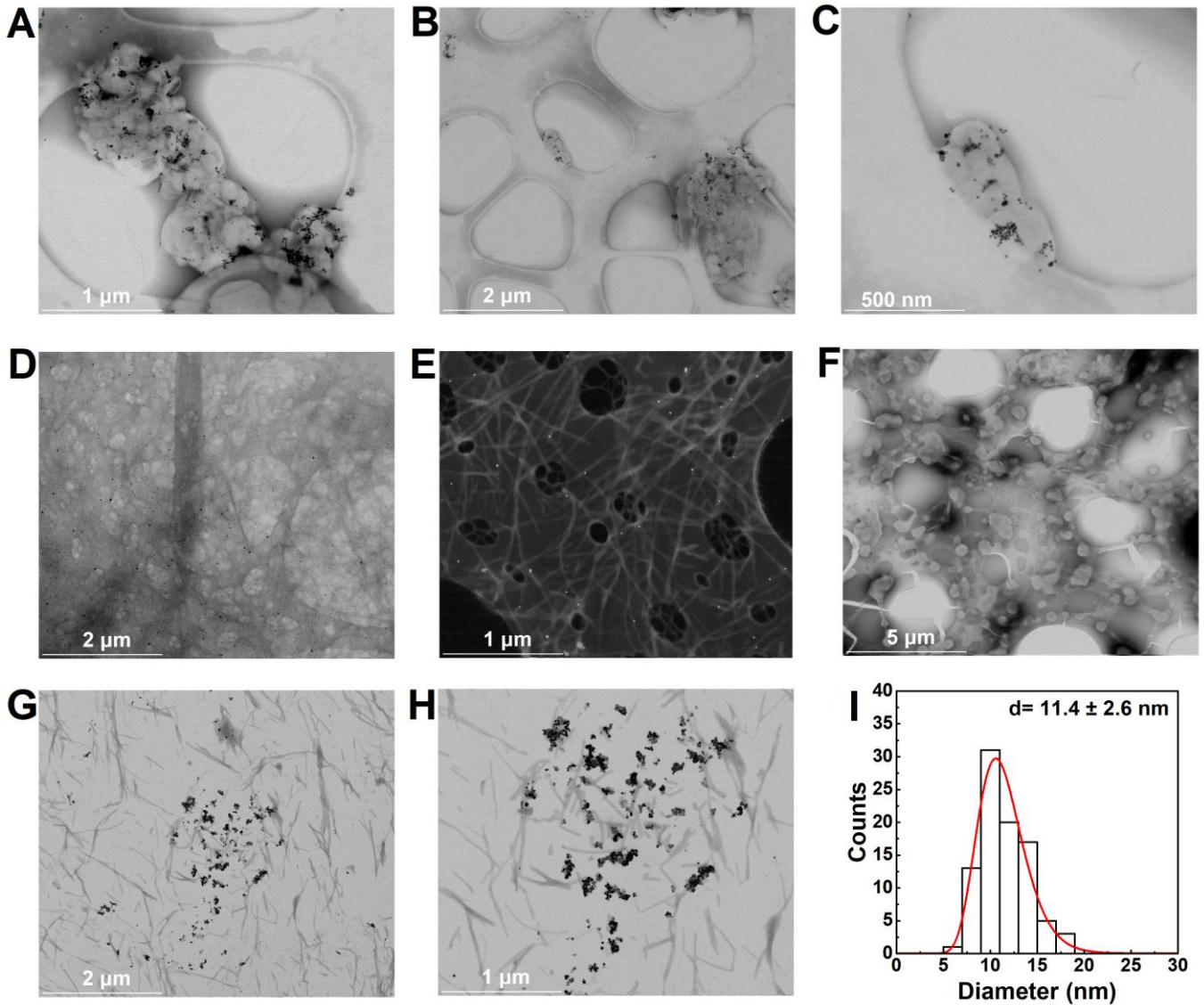
Electron microscopy characterization

Figure S7. Electron microscopy images of: (**A-C**) liposomes of DPPC:DPPE:Ch (8:1:1) (0.1 mM) after interaction with gold nanoparticles (0.4 mM); (**D,E**) lipogel fabricated through the post-mixing method, and (**F**) liposomes observed in the lipogel after applying the contrast agent on the grid; (G,H) lipogel fabricated through the pre-mixing method; (I) Histogram distribution fitted to a lognormal model and calculated average diameter of the gold nanospheres.

The STEM images evidenced the aggregation of gold nanoparticles (~11.4 nm) close to liposomes (figure S7A-C), which is in line with the visually observed aggregation, confirmed through UV-visible absorption spectroscopy, DLS and zeta-potential. The occurrence of gold nanoparticle aggregation on the liposomes surface (including DPPC liposomes) was previously reported by Wang et al.[17-19] The influence of the preparation method (pre- and post-mixing) was also observed through electron microscopy. For instance, the gels obtained through the post-mixing method of preparation (initial mixing of nanoparticles with hydrogel solution and then the mixing with the liposomes solution) resulted in a random distribution of nanoparticles across the gel matrix (figure S7D,E). Interestingly, after addition of the contrast agent to the grid containing the dried gel, it was possible to observe

randomly dispersed liposomes without clearly aggregated nanoparticles nearby (figure S7F). Conversely, the gels obtained through the pre-mixing method displayed the liposome-nanoparticle assemblies (figure S7G,H), that were obtained through the mixing of nanoparticles with the liposomes.
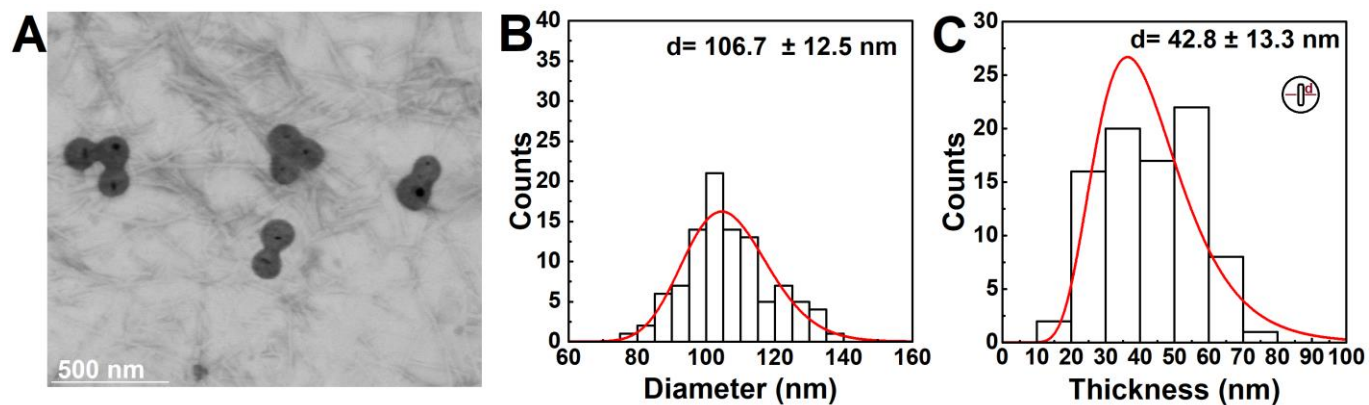

Figure S8. Electron microscopy images of: (**A**) silica-coated nanorods observed in the lipogel after applying the contrast agent on the grid. Histogram distributions fitted to a lognormal model and calculated average (**B**) diameter of the silica-coated gold nanorods and (**C**) silica shell thickness.

Drug release assays

The Gompertz and Korsmeyer-Peppas model is described according to the equations:[44-46]

$$X_t = X_{max} e^{-a e^{b \log_{10} t}} \tag{S1}$$

$$\frac{M_t}{M_\infty} = K_s t^n \tag{S2}$$

in which $\frac{M_t}{M_\infty}$ is the fraction of drug released at time t, and K_s is the rate constant. For a cylindrical geometry, when $n < 0.45$, the release mechanism is diffusion-controlled (Fickian diffusion), $0.45 < n < 0.89$ is an anomalous transport, and $n \geq 0.89$ indicates that the release is mainly driven by swelling or relaxation of network chains (case-II transport). In the former model, X_t and X_{max} are the dissolved fractions at time t and its maximum, a is a shape parameter and b is the dissolution rate per unit of time.

Table S4. Release coefficients of the Korsmeyer-Peppas and Gompertz models obtained for CF release profile from lipogels with non-purified (NP) and purified (P) liposomes (0.5 mM), and from neat hydrogels loaded with 10 µM and 5 µM of CF. The Korsmeyer-Peppas model was fitted to the initial 60% of the drug release profile.

Composites	System	Korsmeyer-Peppas			Gompertz			
		K_S	n	R^2	X_{max}	a	b	R^2
DPPC	NP	0.04421	0.68	0.99	0.47	2.40	0.88	0.99
	P	0.01351	0.74	0.99	0.11	2.17	1.15	0.99
DPPC:DPPE:Ch 8:1:1	NP	0.04470	0.69	0.99	0.37	2.15	1.08	0.99
	P	0.01333	0.69	0.99	0.11	2.26	1.12	0.99
DPPC:DSPE-PEG 19:1	NP	0.04401	0.66	0.99	0.36	2.12	0.99	0.99
	P	0.01113	0.68	0.99	0.29	3.23	0.52	0.98
Neat hydrogel	10 µM CF	0.02419	0.69	0.99	0.38	2.75	0.70	0.99
	5 µM CF	0.03752	0.72	0.99	0.35	2.29	1.05	0.99

Table S5. Release coefficients of the Korsmeyer-Peppas and Gompertz models obtained for CF release profile from hydrogels (10 µM CF) and lipogels with purified liposomes (0.5 mM) and 0.2 mg/mL of silica-coated gold nanorods. The Korsmeyer-Peppas model was fitted to the initial 60% of the drug release profile. The gels were irradiated for 30 min after 24 h and 48 h aliquots with an 808 nm laser intensity of 8 W/cm^2 (R) or xenon arc lamp (200 W) using a Thorlabs FEL0600 long pass filter with cut-on wavelength at 600 nm (L).

| Composites | Stimulus | Korsmeyer-Peppas | | | Gompertz | | | |
		K_S	n	R^2	X_{max}	a	b	R^2
DPPC	None	0.00366	0.77	0.99	0.038	2.39	1.06	0.99
	R	---	---	---	0.053	2.39	0.86	0.93
	L	---	---	---	0.049	2.62	0.91	0.99
DPPC:DPPE:Ch 8:1:1	None	0.00415	0.76	0.99	0.028	2.02	1.53	0.99
	R	---	---	---	0.052	2.41	0.87	0.96
	L	---	---	---	0.038	2.25	1.07	0.98
DPPC:DSPE-PEG 19:1	None	0.00403	0.81	0.99	0.046	2.45	1.07	0.99
	R	---	---	---	0.047	2.37	1.08	0.97
	L	---	---	---	0.055	2.67	0.97	0.99
Hydrogel	None	0.01897	0.71	0.992301	0.225	2.46	0.83	0.98
	R	---	---	---	0.242	2.83	0.87	0.99
	L	---	---	---	0.171	2.35	1.15	0.99

Table S6. Release coefficients of the Korsmeyer-Peppas and Gompertz models obtained for CF release profile from lipogels with purified liposomes (0.5 mM, DPPC:DPPE:Ch 8:1:1) and different concentrations of silica-coated gold nanorods (NR@Si). The Korsmeyer-Peppas model was fitted to the initial 60% of the drug release profile. The gels were irradiated for 15 min or 30 min after 24 h and 48 h aliquots with an 808 nm laser intensity of 8 W/cm^2 or 13 W/cm^2.

| Power (W/cm^2) | NR@Si (mg/mL) | Irradiation time (min) | Korsmeyer-Peppas | | | Gompertz | | | |
			K_S	n	R^2	X_{max}	a	b	R^2
-----	0.2	-----	0.00403	0.81	0.99	0.043	2.42	1.12	0.99
	0.1	-----	0.00424	0.76	0.99	0.048	2.43	0.95	0.98
	0.05	-----	0.00437	0.69	0.99	0.052	2.44	0.76	0.96
8	0.2	30	-----	-----	-----	0.047	2.37	1.08	0.97
	0.1	30	-----	-----	-----	0.054	2.42	0.89	0.95
	0.05	30	-----	-----	-----	0.085	2.88	0.61	0.94
13	0.2	15	-----	-----	-----	0.079	2.63	0.74	0.96
		30	-----	-----	-----	0.107	2.88	0.62	0.93
	0.1	15	-----	-----	-----	0.088	2.82	0.71	0.94
		30	-----	-----	-----	0.074	2.16	0.78	0.94
	0.05	15	-----	-----	-----	0.070	2.69	0.78	0.94
		30	-----	-----	-----	0.068	2.63	0.81	0.95

Drug release assays with gold nanospheres
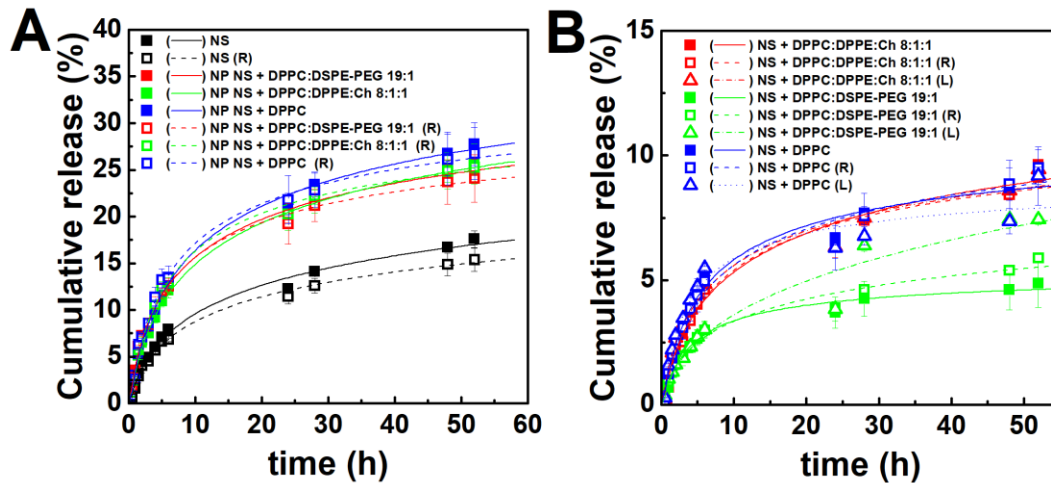
Figure S9. CF release profile from hydrogels (10 µM CF) and lipogels with (**A**) non-purified and (**B**) purified liposomes (0.5 mM) containing gold nanospheres (0.5 mM~0.1 mg/mL). The gels were irradiated for 30 min after 24 h and 48 h aliquots with an 808 nm laser intensity of 8 W/cm^2 (R) or xenon arc lamp (200 W) using a Thorlabs FEL0600 long pass filter with cut-on wavelength at 600 nm (L).

The release from lipogels bearing gold nanospheres (NS) was also assessed, as its plasmonic band is very weakly excited by NIR laser irradiation. Regarding the passive release, the gold nanospheres did not have any major effect over the CF release profiles comparatively to the release from lipogels and hydrogels (Figure 4B, 4C), both in the gels containing non-purified (figure S9A) and purified liposomes (figure S9B), except for the PEGylated formulation that displayed a decrease of the passive release. The lack of hindrance of drug release by the gold nanospheres can be associated with the small particle size (comparable to fibres cross-section) and its negative surface charge. Furthermore, the irradiation with laser or lamp was unsuccessful in inducing an increase of CF release in all samples, compared to the non-irradiated samples, except in the lipogels bearing DPPC:DPPE:Ch 8:1:1 liposomes, that displayed an increase through lamp irradiation. Such could be associated with the weak absorption of the liposome-gold nanosphere aggregates in the NIR wavelength range. Thus, the aggregates do not generate enough heat to induce the phase transition of the liposomes' membrane in all samples as the assays were carried out at room temperature. Besides, the hydrogels containing gold nanospheres also did not achieve any difference compared to the non-irradiated.

Table S7. Release coefficients of the Korsmeyer-Peppas and Gompertz models obtained for CF release profile from hydrogels (10 µM CF) and lipogels with non-purified liposomes (0.5 mM) and gold nanospheres (0.5 mM, ~0.1 mg/mL). The Korsmeyer-Peppas model was fitted to the initial 60% of the drug release profile. The gels were irradiated for 30 min after 24 h and 48 h aliquots with an 808 nm laser intensity of 8 W/cm^2 (R).

Composites	Stimulus	Korsmeyer-Peppas			Gompertz			
		K_S	n	R^2	X_{max}	a	b	R^2
DPPC	None	0.0354	0.75	0.99	0.47	2.65	0.92	0.99
	R	---	---	---	0.37	2.38	1.12	0.99
DPPC:DPPE:Ch 8:1:1	None	0.0336	0.73	0.99	0.48	2.71	0.83	0.99
	R	---	---	---	0.35	2.38	1.14	0.99
DPPC:DSPE-PEG 19:1	None	0.0403	0.67	0.99	0.43	2.39	0.85	0.99
	R	---	---	---	0.35	2.26	1.05	0.99
Hydrogel	None	0.0213	0.75	0.99	0.41	2.93	0.71	0.94
	R	---	---	---	0.32	2.76	0.77	0.99

Table S8. Release coefficients of the Korsmeyer-Peppas and Gompertz models obtained for CF release profile from lipogels with purified liposomes (0.5 mM) and gold nanospheres (0.5 mM, ~0.1 mg/mL). The Korsmeyer-Peppas model was fitted to the initial 60% of the drug release profile. The gels were irradiated for 30 min after 24 h and 48 h aliquots with an 808 nm laser intensity of 8 W/cm^2 (R) or xenon arc lamp (200 W) using a Thorlabs FEL0600 long pass filter with cut-on wavelength at 600 nm (L).

Composites	Stimulus	Korsmeyer-Peppas			Gompertz			
		K_S	n	R^2	X_{max}	a	b	R^2
DPPC	None	0.0129	0.78	0.99	0.12	1.13	2.27	0.98
	R	---	---	---	0.15	0.87	2.38	0.96
	L	---	---	---	0.09	1.34	1.84	0.94
DPPC:DPPE:Ch 8:1:1	None	0.0115	0.79	0.99	0.18	0.79	2.68	0.97
	R	---	---	---	0.13	1.02	2.55	0.98
	L	---	---	---	0.15	0.86	2.31	0.97
DPPC:DSPE-PEG 19:1	None	0.0085	0.72	0.99	0.06	1.33	1.95	0.98
	R	---	---	---	0.13	0.63	2.59	0.97
	L	---	---	---	1	0.34	4.65	0.90

Photothermia assays

Regarding the optimization of the irradiation parameters, different concentrations of silica-coated gold nanorods were initially irradiated with an 808 nm laser (13 W/cm^2) as illustrated in figure S10A, which depicts the concentration dependence of the heating process. The temperature strongly increased in the first 10 min and slowly increased hereafter. Besides, the sample could reproduce the heating profiles over several on/off cycles (figure S10B). To improve the maximum temperature, the experimental setup was optimized by changing the laser focus (figure 6C) as a means to modify the power density on the sample from 27 W/cm^2 to 1 W/cm^2. Despite the high-power density, the small irradiation radius was detrimental for the assessed samples, as the amount of excited nanorods is diminished. The best outcome was achieved for 3 W/cm^2, providing a good balance of power density and amount of sample that is covered. Hence, these optimized experimental parameters were also tested for other nanoparticle concentrations (Figure 5).
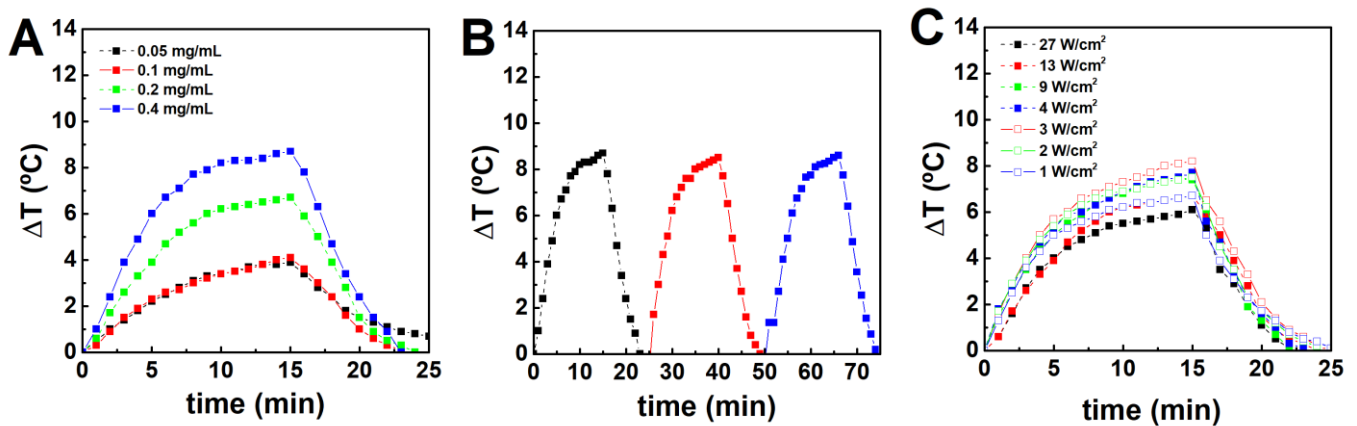

Figure S10. Temperature variation of AuNRs coated with mesoporous silica: (**A**) with different concentrations upon 808 nm laser irradiation (13 W/cm^2) with an output of 800 mW; (**B**) for three on/off cycles at 13 W/cm^2 for a concentration of 0.4 mg/mL; (**C**) with different intensity by varying the laser focus.

Table S9. Release coefficients of the Korsmeyer-Peppas and Gompertz models obtained for CF release profile from lipogels with purified liposomes (0.5 mM) and 0.2 mg/mL of silica-coated gold nanorods. The Korsmeyer-Peppas model was fitted to the initial 60% of the drug release profile. The gels were continuously irradiated for 6 h with an 808 nm laser intensity of 3 W/cm^2 (R).

	Korsmeyer-Peppas			Gompertz			
Stimulus	K_S	n	R^2	X_{max}	a	b	R^2
None	0.0122	0.61	0.99	0.06	1.65	1.36	0.99
R	0.0229	0.44	0.99	0.44	2.95	0.39	0.99

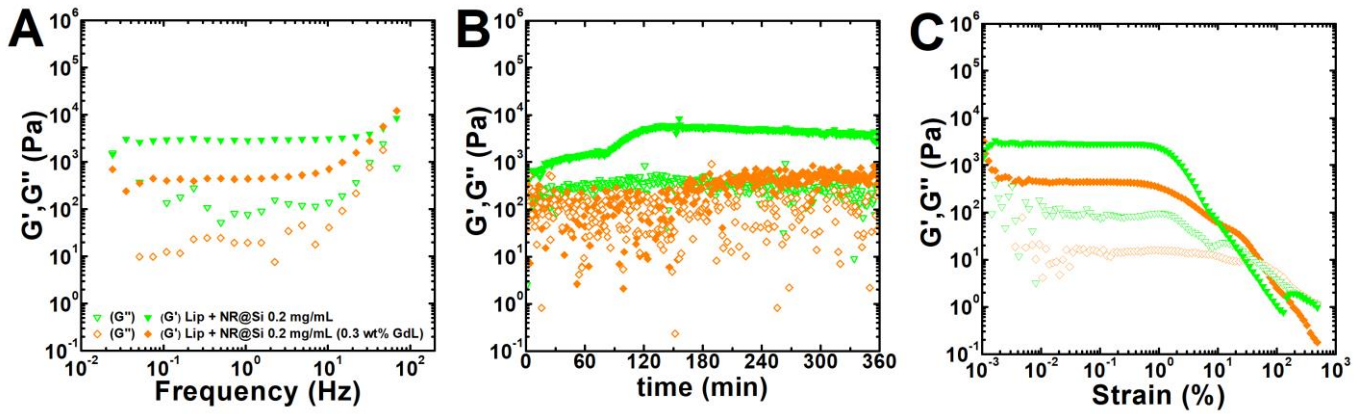# Rheological properties of plasmonic lipogels

Figure S11. (**A**) Shear storage G' (filled symbols) and loss G'' (empty symbols) modulus during the frequency sweep of hydrogel (0.5 wt% hydrogelator; 0.3 wt% GdL) bearing silica-coated gold nanorods (AuNRs) at 0.2 mg/mL, and liposomes (Lip AuNRs, 0.5 mM). The frequency sweep of the liposome-containing hydrogel at 0.4 wt% of GdL and with 0.2 mg/mL of nanoparticles is also included. Comparison of (**B**) gelation kinetics and (**C**) strain sweep of liposome-containing hydrogels with 0.2 mg/mL of nanoparticles prepared with 0.4 wt% and 0.3 wt% of GdL.